View Article Online / Journal Homepage / Table of Contents for this issue

Coordination of substitutionally inert phenolate ligands to lanthanide(II) and (III) compounds—catalysts for ring-opening polymerization of cyclic esters†

Pascal I. Binda,[a] Ewan E. Delbridge,*[b] Harmon B. Abrahamson*[a] and Brian W. Skelton[c]

Received 4th December 2008, Accepted 26th January 2009
First published as an Advance Article on the web 23rd February 2009
DOI: 10.1039/b821770j

Published on 23 February 2009 on http://pubs.rsc.org | doi:10.1039/B821770J
Downloaded by UNIVERSITY OF BRIGHTON on 30/04/2013 12:15:14.

A new [ONO] tridentate phenolate ligand (H_2L^I) containing an aliphatic alcohol as a side arm has been synthesized, deprotonated and attached to lanthanide(II) and (III) ions, which are employed as catalysts for ring-opening polymerization of cyclic esters. In contrast to many other mono-phenolate lanthanide compounds, these have been found to be inert to polymer incorporation during the polymerization reactions. Three new divalent ytterbium compounds have been synthesized in high yield containing ancillary ligands; two *via* a transamination reaction between $[Yb(N(SiMe_3)_2)_2(THF)_2]$ and one equivalent of the phenols, HOC_6H_2-(2,4-^{t}Bu)-6-$CH_2N(Me)CH_2CH_2OH$ (H_2L^I) or HOC_6H_2-(2,4-^{t}Bu)-6-$CH_2N(Me)CH_2CH_2N(Me)CH_2$-6-(2,4-^{t}Bu)-$C_6H_2OH$ (H_2L^{II}) in hexanes to yield $[Yb(L^I)]_2$ (**1**) and $[Yb(L^{II})]_2$ (**2**), respectively. The third divalent ytterbium compound $[Yb(L_2)]$ (**3**) was prepared by treatment of $[Yb(N(SiMe_3)_2)_2(THF)_2]$ with two equivalents of a related monoanionic ancillary phenol, HOC_6H_2-(2,4-^{t}Bu)-6-$CH_2N(Me)CH_2CH_2NMe_2$ (HL) in hexanes. Additionally, the oxidation chemistry of these divalent systems was explored where compound **1** was treated with silver triflate and phenol to form corresponding heteroleptic trivalent ytterbium phenolate complexes $[Yb(L^I)(O_3SCF_3)(THF)]$ (**4**) and $[Yb(L^I)(OPh)]$ (**5**), respectively. Finally, three new heteroleptic trivalent lanthanide silylamido compounds were synthesized *via* a ligand exchange transamination reaction between the homoleptic trivalent $[Ln(N(SiMe_3)_2)_3]$ compound and one equivalent of the new dianionic ligand (H_2L^I) in THF $\{[La(L^I)(N(SiMe_3)_2)(THF)_2]$ (**6**); $[Sm(L^I)(N(SiMe_3)_2)(THF)]$ (**7**); $[Yb(L^I)(N(SiMe_3)_2)(THF)]$ (**8**)$\}$. These lanthanide(II) and (III) compounds were assessed as catalyst precursors towards the ring-opening polymerization of both L-lactide and ε-caprolactone. End-group analyses and detailed kinetics studies {rate law: $-d[LA]/dt = k[LA]^1[catalyst]^1$} of the most efficacious lanthanum compound (**6**) further corroborated the substitutionally inert characteristics of the new stationary ancillary [ONO] tridentate dianionic ligand.

Introduction

Recent developments in the synthesis and applications of lanthanide complexes have focused on the use of non-cyclopentadienyl (Cp) ligands containing multidentate anionic ligands such as guanidinate,[1–4] β-diketiminates,[5–8] salen,[9,10] diamides[11,12] and bis(phenolates).[13–18] This is primarily because these ligands are easily tunable; a unique feature, which allows for the convenient variation of the steric and electronic properties, making them less susceptible to ligand redistribution reactions compared with their Cp counterparts. As a result, lanthanide compounds have found great utility in catalysis,[14,19–22] fluorescence,[19,23–28] agriculture[29] and redox chemistry.[19,30] Among these ligand systems, lanthanide compounds containing multidentate and often multianionic phenolate and bis(phenolate) ligands have recently exhibited excellent catalytic properties towards the ring-opening polymerization (ROP) reactions of cyclic esters such as lactide (LA) and ε-caprolactone (ε-CL).[9,14,16–18,31–37] The significant chelating ability of such ligands to oxophilic lanthanides renders these substrates substantially inert to substitution during the polymerization reaction; an often sought after property where stereochemical control of the polymerization of *rac*-lactide is desired. As such, there is continued interest in the architecture and binding stability of such multidentate ligands as stationary 'spectator' ligands in ROP research.

The authors' recent studies have focused on the use of potential monoanionic phenolate ligand (HL) (Fig. 1) to stabilize lanthanide metals during ROP of cyclic esters.[37] The choice of this system was motivated by the hypothesis that monoanionic multidentate (HL) ligands could provide an optimal balance between ligand conformational flexibility and substitutionally inert characteristics, if compared to a typical unidentate PhO^- and more encumbered multidentate ligands. However these previous studies revealed unanticipated lability of L^- ligand during ROP reactions such that the multidentate, monoanionic phenolate

[a]*Chemistry Department, University of North Dakota, Grand Forks, ND 58202-9024, USA. E-mail: habrahamson@chem.und.edu; Fax: +1 701 777 2331; Tel: +1 701 777 4427*
[b]*The Lubrizol Corporation, Wickliffe, OH 44092, USA. E-mail: ewan.delbridge@lubrizol.com; Fax: +1 440 347 4713; Tel: +1 440 347 1535*
[c]*The University of Western Australia, School of Biomedical, Biomolecular and Chemical Sciences, Chemistry M313, Crawley, 6009/, Western, Australia. E-mail: brian.skelton@uwa.edu.au; Fax: +61 08 6488 1118; Tel: +61 08 6488 7107*

† Electronic supplementary information (ESI) available: Mass spectrum, ^{1}H NMR spectra, ORTEP diagram, ROP mechanism and second-order kinetics plot for L-lactide *vs.* time. CCDC reference numbers 711938. For ESI and crystallographic data in CIF or other electronic format see DOI: 10.1039/b821770j

Published on 23 February 2009 on http://pubs.rsc.org | doi:10.1039/B821770J
Downloaded by UNIVERSITY OF BRIGHTON on 30/04/2013 12:15:14.

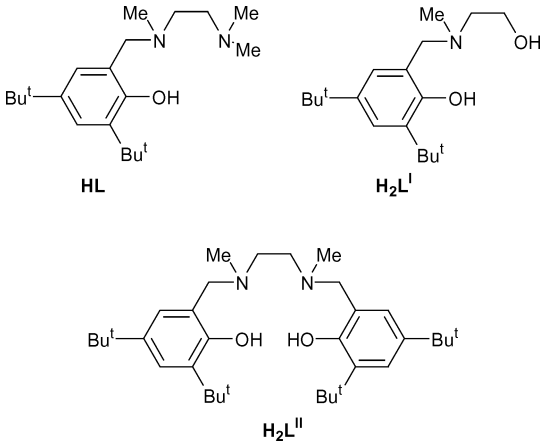

Fig. 1 Multidentate ancillary phenolate ligands.

ligand did not remain bound to the lanthanide metal center but rather it was incorporated into the polymer, making it an effective polymerization initiation group.[37] It was rationalized that the lanthanide metal forms only weakly dative bonds with the hindered tertiary amine, NMe_2 side arm in ligand (L^-).[37] In order to circumvent this problem, we decided to rebuild and tune the ligand architecture by substituting the poorly coordinating NMe_2 side arm for a readily deprotonatable aliphatic alcohol or another phenol to afford two dianionic ligand variants, H_2L^I and H_2L^{II}, respectively (Fig. 1). Reported herein is the synthesis and characterization of divalent and trivalent lanthanide complexes, supported by potentially tridentate [ONO] (H_2L^I) and tetradentate [ONNO] (H_2L^{II}) dianionic phenolate ligands, and their reactivity towards L-lactide and ε-caprolactone.

Results and discussion

Design and synthesis of stationary spectator ligands

Due to the previously reported[37] lability of the ligand HOC_6H_2-(2,4-^{t}Bu)-6-$CH_2N(Me)CH_2CH_2NMe_2$ (Fig. 1; HL) we decided to rebuild and tune the ligand architecture by modification of the NMe_2 side arm to: (1) an aliphatic alcohol to afford a potentially tridentate [ONO] dianionic ligand, HOC_6H_2-(2,4-^{t}Bu)-6-$CH_2N(Me)CH_2CH_2OH$ (H_2L^I); and (2) another phenol to afford a bis(phenolate) [ONNO] potentially tetradentate dianionic ligand, HOC_6H_2-(2,4-^{t}Bu)-6-$CH_2N(Me)CH_2CH_2N(Me)CH_2$-6-(2,4-^{t}Bu)-$C_6H_2OH$ (H_2L^{II}) (Fig. 1). The ligands HL and HL^{II} were synthesized *via* reported procedures[38,39] while the new ligand 2,4-di-*tert*-butyl-6-{[(2′-hydroxyethyl)-ethylamino]methyl}phenol (H_2L^I) was analogously synthesized from 2,4-di-*tert*-butylphenol, formaldehyde and 2-(methylamino)ethanol (Scheme 1) and fully characterized *via* established methods (^1H and $^{13}C\{^1H\}$ NMR, IR spectroscopy, ESI mass spectrometry and elemental analysis (see ESI Fig. S1 and S2).† These ligands were subsequently utilized in the syntheses of divalent and trivalent lanthanide compounds, catalyst precursors for the ROP of cyclic esters.

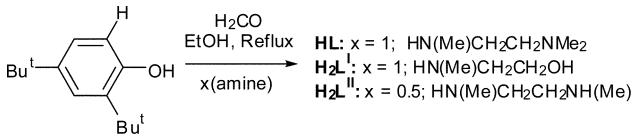

Scheme 1 Synthesis of ancillary ligands *via* Mannich condensations.

Synthesis of lanthanide compounds

Synthesis of divalent ytterbium compounds. Three new divalent ytterbium compounds **1–3** have been synthesized in high yield, *via* acid–base transamination reactions employing one equivalent of the ytterbium precursor, $[Yb(N(SiMe_3)_2)_2(THF)_2]$ and either one equivalent of the ligands H_2L^I and H_2L^{II} in hexanes to afford $[YbL^I]_2$ (**1**) and $[YbL^{II}]_2$ (**2**), or two equivalents of HL to afford, YbL_2 (**3**) in hexanes (Scheme 2).

The divalent ytterbium compounds **1–3** have been fully characterized by NMR and IR spectroscopy, elemental analysis and melting point (see Experimental). Both ^1H and $^{13}C\{^1H\}$ NMR spectroscopy of compounds **1** and **2** in C_7D_8 revealed two distinct ligand environments (in approximate equal ratio); likely caused by molecular oligomerization to satisfy the coordinatively unsaturated ytterbium atoms. However, NMR spectroscopy of **1** and **2** in the presence of a donor solvent (C_4D_8O), revealed only one chemical environment consistent with a symmetrical, coordinatively saturated, monomeric ytterbium center. This solution behaviour exhibited by compounds **1** and **2** has been well documented for ytterbium(II) compounds with coordinated ancillary, dianionic ligands.[13,18] X-Ray crystallography of deep-red single crystals of **2**, grown from a toluene–hexanes mixture at –20 °C, indeed supported a dimeric, divalent, five-coordinate ytterbium arrangement where the fifth coordination site arises from a bridging phenolic oxygen of the second ligand (see Fig. 3, Table 1 and X-ray crystallographic discussion below). Interestingly, agostic interactions between the ^{t}Bu protons and

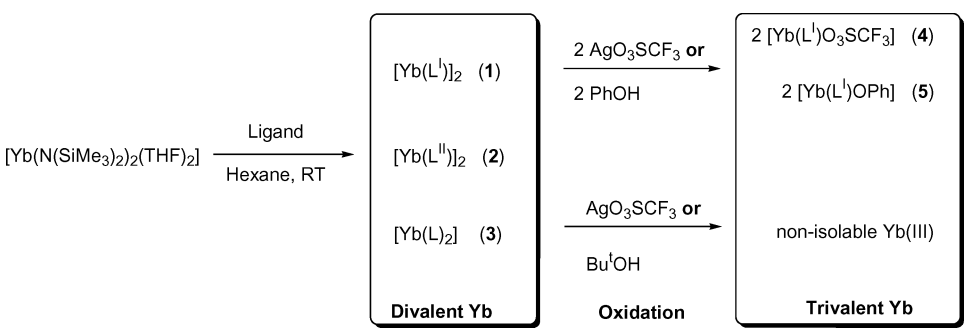

Scheme 2 Synthesis of ytterbium(II) and (III) ancillary phenolate compounds.

 This journal is © The Royal Society of Chemistry 2009

Downloaded by UNIVERSITY OF BRIGHTON on 30/04/2013 12:15:14.
Published on 23 February 2009 on http://pubs.rsc.org | doi:10.1039/B821770J

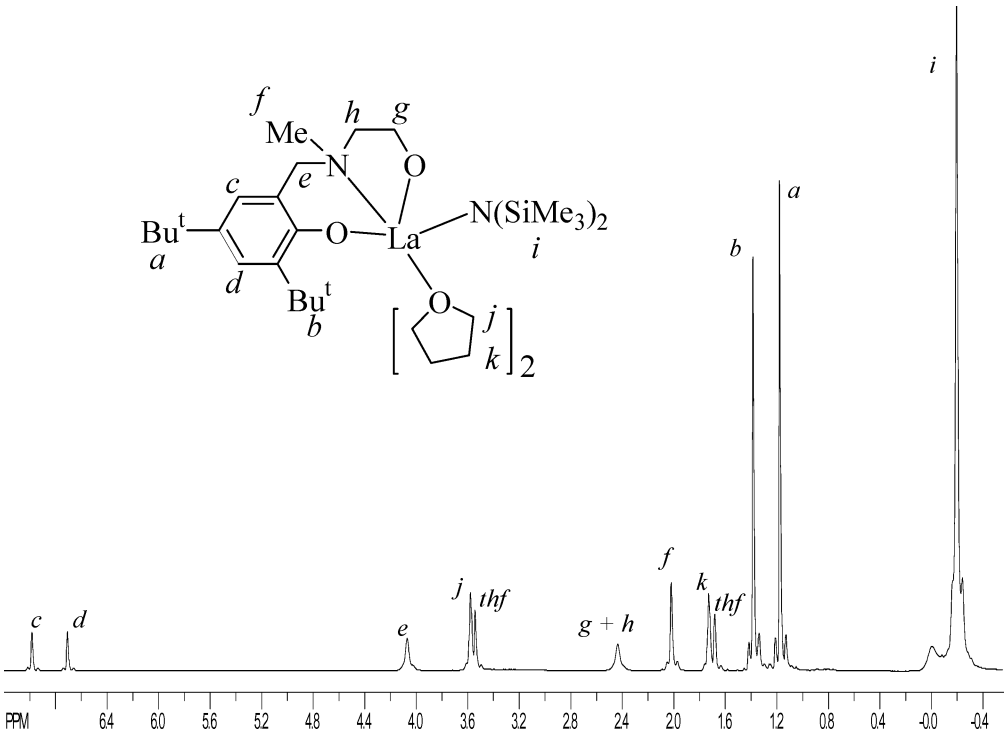

Fig. 2 ^{1}H NMR spectrum of compound **6** in C_4D_8O at 70 °C.

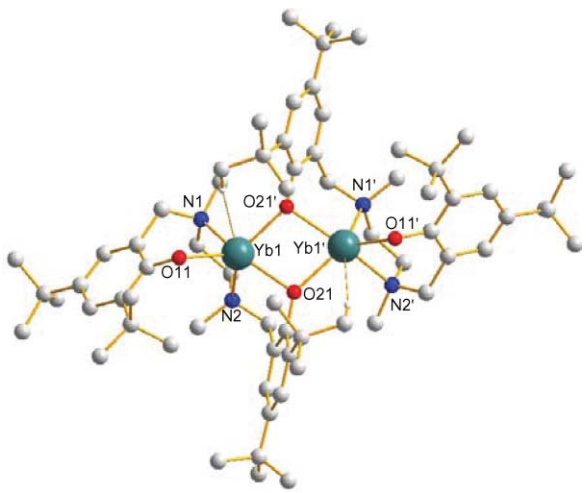

Fig. 3 Molecular representation of compound **2** (hydrogen atoms and the toluene solvent molecules have been omitted). Primed atoms are generated by the 2-fold axis.

ytterbium (see below discussion) are preserved in solution; as indicated in the ^{1}H NMR spectrum of **2** in C_7D_8 where the agostic proton(s) are somewhat deshielded (2.3 *vs.* 1.8 ppm, see ESI Fig. S3).†

Conversely, the ^{1}H NMR spectrum of compound **3** demonstrated a symmetric arrangement of both L ligands in either donor or non-donor solvents; indicative of a monomeric solution structure. Undoubtedly, steric constraints impose a monomeric ytterbium structure since two conformationally flexible monoanionic ligands (L) are required to satisfy charge, which completely fill the coordination sphere about ytterbium.

Table 1 Ytterbium atom environments in compound **2**

Yb(1)	*r*/Å	O(21)	O(21′)	N(1)	N(2)
O(11)	2.2153(17)	127.47(6)	129.65(6)	84.46(7)	102.88(7)
O(21)	2.3650(16)		77.31(6)	142.77(6)	81.80(6)
O(21′)	2.3143(16)			97.38(6)	125.53(6)
N(1)	2.537(2)				71.45(7)
N(2)	2.532(2)				

Yb(1)···Yb(1′) 3.6393(2) Å. *r*/Å is the ytterbium–ligand atom distance; other entries in the matrix are the angles (°) subtended at the ytterbium atom by the relevant atoms at the head of the row and column. Primed atoms are generated by $1 - x, y, 3/2 - z$.

Oxidation of divalent ytterbium compounds. Trivalent heteroleptic lanthanide complexes are often synthesized *via* proton exchange reactions involving appropriate homoleptic starting materials, such as $[Ln(N(SiHMe_2)_2)_3(THF)_2]$, $[Ln(N(SiMe_3)_2)_3]$ or $[Ln(CH_2Ph)_3(THF)_3]$, and ligands possessing sufficiently acidic protons available to affect a ligand exchange.[35,37,40] However, lanthanide compounds possessing an accessible divalent oxidation state, such as ytterbium, offer an alternate synthetic pathway to heteroleptic complexes by reaction of the ytterbium(II) compound with mild oxidizing agents such as AgO_3SCF_3, ROH (aliphatic), PhOH, TlCp and $AgPF_6$.[13,18,30]

Divalent ytterbium compounds **1** and **3** were treated with different oxidants to obtain a variety of trivalent ytterbium compounds **4** and **5** (Scheme 2) having LLnX formulations. These motifs represent ideal candidates for coordination/insertion catalyst precursors for the ring-opening polymerization of cyclic esters, where L is a stationary ancillary ligand, Ln is a lanthanide metal and X is a labile initiating group. The divalent ytterbium dimeric compound **1** was readily oxidized with an equivalent (based on Yb)

Published on 23 February 2009 on http://pubs.rsc.org | doi:10.1039/B821770J
Downloaded by UNIVERSITY OF BRIGHTON on 30/04/2013 12:15:14.

of silver triflate and phenol to obtain [Yb(L^{I})(O$_3$SCF$_3$)(THF)] **4** and [Yb(L^{I})(OPh)] **5**, respectively.

Compounds **4** and **5** were characterized by elemental analysis, melting point and IR spectroscopy. NMR spectroscopic analyses were not feasible due to the highly paramagnetic properties of trivalent ytterbium.[13,18,37] However, satisfactory elemental analyses of **4** suggested a molecule of THF present in the formulation.

Repeated attempts to obtain X-ray quality single crystals of these compounds were unsuccessful. However, compound **4** likely has a similar structure to the previously reported analogous heteroleptic ytterbium(III) phenolate triflate compound, containing a six-coordinate ytterbium center with quasi-octahedral geometry comprising a bidentate coordination of the triflate ligand.[13]

Oxidation of compound **3** with silver triflate or tertiary butanol yielded un-isolable products; likely resulting in a mixture of disproportionated heteroleptic compounds.[37] Despite a significant colour change from dark green to pale yellow, indicative of successful oxidation of Yb(II) to Yb(III), repeated attempts to obtain analytically pure samples were unsuccessful.

Synthesis of trivalent lanthanide phenolate compounds by ligand exchange reactions. Access to trivalent heteroleptic lanthanide complexes containing silylamides (as the initiating group) were readily obtained by ligand exchange reactions between the homoleptic [Ln(N(SiMe$_3$)$_2$)$_3$] compounds and H$_2$L^{I} in THF to afford three new lanthanide compounds: [La(L^{I})(N(SiMe$_3$)$_2$)(THF)$_2$] (**6**), [Sm(L^{I})(N(SiMe$_3$)$_2$)(THF)] (**7**), [Yb(L^{I})(N(SiMe$_3$)$_2$)(THF) (**8**) (Scheme 3).

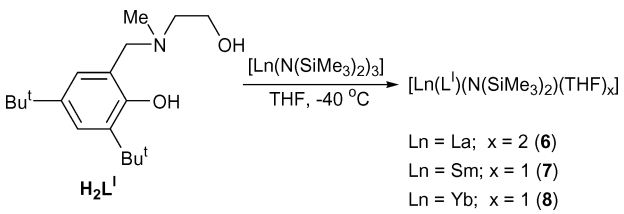

Scheme 3 Synthesis of Ln(III) compounds *via* transamination reactions.

The lanthanide compounds **6–8** have been fully characterized by NMR and IR spectroscopy, elemental analysis and melting point, except for the paramagnetic ytterbium compound **8**, where no satisfactory NMR spectroscopic data were obtained (see Experimental). NMR spectroscopic and elemental analyses data is suggestive that the lanthanum compound, **6**, contains two THF molecules whilst the samarium analogue, **7**, contains only one THF molecule in the formulation. If these THF molecules are coordinated to the metal center, these formulations are consistent with the relative ionic radii of the larger La *vs.* the smaller Sm. The room temperature ^{1}H NMR spectrum of compound **6** in C$_4$D$_8$O displayed broadened methylene and NMe protons that sharpened as the temperature was raised (see Fig. 2, Experimental and ESI Fig. S4).† Elemental analysis of compound **8** also supports the presence of one THF molecule. The proposed formulations of compounds **6–8** were further established by comparison of the THF signals found in the ^{1}H NMR spectra of compounds **6** and **7** C$_6$D$_6$ to those observed in an NMR spectrum of neat THF in C$_6$D$_6$. A discernible downfield shift of the α-protons (from 3.53 to 3.60 and 3.56 ppm for **6** and **7**, respectively) is observed upon THF coordination to the lanthanide metal centers. A similar, but less pronounced effect, was observed for the β-THF protons. These results imply that tridentate coordination of the stationary ligand is likely since the coordination sphere in these compounds is unsaturated and completed by THF coordination, suggesting that this stationary ligand would remain bound to the metal center during any ROP reactions.

Numerous attempts to grow X-ray quality single crystals were thwarted such that definitive solid-state structural data was not available. Furthermore, no mass spectral data were obtained for these highly air- and moisture-sensitive compounds.

X-Ray crystallography of 2

The results from the single-crystal X-ray structural determination of **2** report a dimeric structure with bridging and terminal phenolate ligands consistent with the [Yb(L^{II})]$_2$ formulation (Fig. 3 and Table 1). The recently reported La(III) bis(phenolate),[41] also dimeric, displays structural similarities to [Yb(L^{II})]$_2$, which is expected given the larger size of lanthanum being able to accommodate a bridging ligand arrangement. Both elemental and the ^{1}H NMR spectroscopic analyses support the solid-state formulation (see above Discussion); the latter collected in C$_7$D$_8$ promoting magnetically inequivalent phenolate ligand environments in non-donor solvents. Additionally, the solid-state structure (Fig. 3) proposes an agostic interaction between one (^{t}Bu) group of the ligand and the ytterbium metal [Yb(1)$\cdots$H(26A) (1 – x, y, 3/2 – z) 2.71 Å], which appears to be preserved in solution (see above) also destroying the C_2-symmetry of the bis(phenolate) ligand. Agostic interactions between lanthanide metals and alkyl/aryl hydrogen atoms are well established in the literature[42] and support the credibility of the interaction reported herein.

The dimeric structure is generated by the crystallographic 2-fold axis along *b*. There are also two toluene molecules per dimer. The central Yb$_2$O$_2$ ring deviates from planarity with the angle between the two YbO$_2$ planes being 10.41(7)°. Each ytterbium atom is five-coordinate; a η^4-bis(phenolate) occupying four coordination sites and the fifth obtained from a bridging phenolic oxygen of the the other bis(phenolate) ligand (see ESI Fig. S5 for thermal ellipsoid plot).† The ytterbium coordination environments in **2** display distorted trigonal bipyramidal geometry possessing metrical similarities to recently reported five-coordinate ytterbium(II) bis(phenolate) compounds[13] and as such, no detailed discussion of bond lengths and angles are presented herein (see Table 1 and Fig. 3). As typical with these compounds, steric bulk of the bis(phenolate) [ONNO] ligand stabilizes the somewhat low coordination number of the ytterbium(II) center.

Polymerization studies using lanthanide compounds

Compounds **1–8** reported herein have been assessed as catalyst precursors in ring–opening polymerization of cyclic esters, *i.e.*, ε-caprolactone and L-lactide. Polycaprolactone and polylactide are among a growing number of 'green' polyesters derived from renewable resources which continue to receive significant attention because of their numerous applications ranging from packaging to drug delivery materials.[43–57]

Recently, the authors reported the lability of the multidentate monoanionic phenolate ligand (L) (Fig. 1) coordinated to Ln(III) ions (Ln = La, Sm and Yb) during ROP of cyclic

 This journal is © The Royal Society of Chemistry 2009

Downloaded by UNIVERSITY OF BRIGHTON on 30/04/2013 12:15:14.
Published on 23 February 2009 on http://pubs.rsc.org | doi:10.1039/B821770J

esters and its incorporation into polymer chains (*via* activation during polymerization initiation).[37] The current study expands on these initial findings *via* catalyst refinement by way of ligand modification (*i.e.* H_2L^I and H_2L^{II}, Fig. 1). The principal objective of this study was to investigate two effects: (1) How stationary 'spectator' ligand redevelopment would affect polymerization dynamics (*i.e.*, reaction kinetics, polymer composition, *etc.*); (2) comparison of lanthanide(II)/(III) catalyst efficacy towards ring-opening polymerization of cyclic esters.

The outcomes from these studies, discussed below in detail, reveal the following: (1) the modified phenolate ligand $[(L^I)^{2-}]$ remains bound to the lanthanide metal center during polymerization reactions, in contrast to the monoanionic phenolate ligand $[(L)^{1-}]$;[37] (2) the more substitutionally inert $(L^I)^{2-}$ ligand influences catalyst activity, most notably in ytterbium catalysts; (3) catalyst precursors containing larger lanthanide metals polymerize cyclic esters more rapidly than those containing smaller, heavier lanthanides; (4) lanthanide catalyst precursors polymerize caprolactone more readily than lactide, and (5) the rate law (obtained *via* compound **6** and L-LA polymerization systems) obeys: $-d[LA]/dt = k[monomer]^1[catalyst]^1$, which is first-order in monomer and first-order in catalyst precursor in contrast to the previously reported $[La(L)_2(N(SiMe_3)_2)]$,[37] which was second-order in lactide.

Ytterbium(II) phenolate catalyst precursors 1–3. The homoleptic divalent ytterbium phenolates, compounds **1–3**, had difficulty polymerizing both L-lactide and ε-caprolactone (Tables 2 and 3, respectively; entries 1–3) even at elevated temperature (80 °C). However, catalyst precursor **3** displayed superior polymer conversion in both lactide (80 °C) and caprolactone (room temperature) polymer systems yielding 63 and 76%, respectively, whilst catalyst precursors **1** and **2** yielded no detectable polylactide and only 47 and 45% polycaprolactone conversions (80 °C), respectively, within 60 min. These polymer conversion data for **3** are comparable to those reported[37] for the trivalent ytterbium phenolate amido catalyst precursor $[Yb(L_2)(N(SiMe_3)_2)]$ (59% for both polylactide (80 °C) and polycaprolactone (room temperature). Near instantaneous oxidation (observable by reaction colour change) of the ytterbium(II) center in **3**, in the presence of monomer substrates, presumably affords a "$Yb^{III}L_2X$" species, similar in motif to the previously reported amide, where X is a ring-opened monomer *i.e.* a propagating alkoxide group. Thus it would be anticipated that if $k_{initiation} >> k_{propagation}$ (highly plausible) similar polymer conversions for these two catalyst systems would be observed since initiation would not be rate-determining. Additionally, polycaprolactone polydispersity was higher for reactions employing catalyst precursor **3** *vs.* **1** (1.52 *vs.* 1.26, respectively; Table 3, entries 1 and 3) despite higher reaction temperatures being employed in the latter. This is consistent with **1** comprising a more substitutionally inert dianionic 'spectator' phenolate ligand which suppresses transesterification side reactions (see below for more detailed discussion of catalysts employing this dianionic, monophenolate ligand systems).

Ytterbium(III) phenolate catalyst precursors 4, 5 and 8 containing the dianionic phenolate ligand L^I. Compounds **4**, **5** and **8**, the trivalent counterparts to **1**, were insufficiently active to appreciably polymerize the monomers L-lactide or ε-caprolactone within 60 min at 80 °C. However, longer reaction times (8–24 h), under similar reaction conditions, did produce polylactide and polycaprolactone, albeit at modest conversion (43–61% polymer conversion) using compounds **5** and **8** whilst compound **4** was totally inactive (Table 2; entries 4–5 and Table 3; entries 4–6). Additionally, complete monomer conversion was not obtained with compounds **5** and **8**, even at extended reaction times (days), which may simply reflect polymerization termination *via* hydrolysis derived from adventitious moisture (see ESI Fig. S6).† This lack of reactivity is reminiscent of that observed for the divalent ytterbium catalyst precursor **1**, merely reflecting a similar restrictive coordination environment about ytterbium metal that is less able to accommodate an incoming monomer substrate; a necessary requirement for effective ROP *via* the widely proported coordination–insertion mechanism (see ESI Fig. S6).† Moreover,

Table 2 Results of polymerization of L-LA in toluene at room temperature

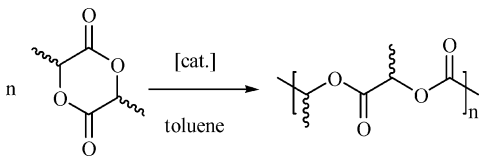

Entry	Initiator [cat.]	[M]/[I][a]	Time/min	Conv. (%)[b]	M_n (x 10^4)[c]	PDI[c]
1	L^IYb **1**	100	60[d]	0	—	—
2	$L^{II}Yb$ **2**	100	60[d]	0	—	—
3	L_2Yb **3**	100	60[d]	63	0.91	1.27
4	L^IYbOPh **5**	100	24 h[d]	57	—	—
5	$L^IYbN(SiMe_3)_2(THF)$ **8**	100	24 h[d]	61	—	—
6	$L^ILaN(SiMe_3)_2(THF)_2$ **6**	100	1	94	2.35	1.23
7	$L^ILaN(SiMe_3)_2(THF)_2$ **6**	100	10	97	2.26	1.62
8	$L^ILaN(SiMe_3)_2(THF)_2$ **6**	200	10	96	—	—
9	$L^ILaN(SiMe_3)_2(THF)_2$ **6**	500	10	95	—	—
10	$L^ILaN(SiMe_3)_2(THF)_2$ **6**	1000	10	94	—	—
11	$L^ISmN(SiMe_3)_2(THF)$ **7**	100	60[d]	35	0.525	1.01

[a] Monomer to initiator ratio. [b] Conversion: determined by ^1H NMR spectroscopy. [c] Determined by gel permeation chromatography (GPC) with calibration to polystyrene standards. [d] Temperature at 80 °C.

View Article Online

Table 3 Results of polymerization of ε-CL in toluene at room temperature

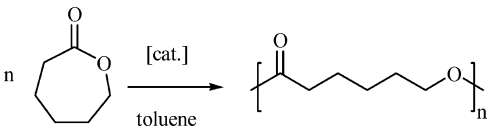

Entry	Initiator [cat.]	[M]/[I][a]	Time/min	Conv.[b] (%)	M_n(x 10^4)[c]	PDI[c]
1	L^1Yb **1**	100	60[d]	47	0.60	1.26
2	L^{II}Yb **2**	100	60[d]	45	—	—
3	L_2Yb **3**	100	60	76	0.61	1.52
4	$L^1YbO_3SCF_3(THF)$ **4**	100	60[d]	0	—	—
5	L^1YbOPh **5**	100	8 h[d]	45	—	—
6	$L^1YbN(SiMe_3)_2(THF)$ **8**	100	8 h[d]	43	—	—
7	$L^1LaN(SiMe_3)_2(THF)_2$ **6**	100	1	100	1.63	1.34
8	$L^1SmN(SiMe_3)_2(THF)$ **7**	100	10	62	—	—
9	$L^1SmN(SiMe_3)_2(THF)$ **7**	100	30	77	—	—
10	$L^1SmN(SiMe_3)_2(THF)$ **7**	100	60	78	0.83	1.11

[a] Monomer to initiator ratio. [b] Conversion: determined by ^{1}H NMR spectroscopy. [c] Determined by gel permeation chromatography (GPC) calibrated to polystyrene standards. [d] Temperature at 80 °C.

Downloaded by UNIVERSITY OF BRIGHTON on 30/04/2013 12:15:14.
Published on 23 February 2009 on http://pubs.rsc.org | doi:10.1039/B821770J

poor nucleophilicity of the triflate ion in **4**, steric crowding promoted by the OPh initiating group in **5** coupled with a smaller lanthanide ion, ytterbium, also likely contribute to this lack of catalytic activity.[13,31]

However, this decreased reactivity of ytterbium catalyst systems containing dianionic monophenolate L^1 *vs.* monoanionic monophenolate L highlights the former ligand's superior chelating ability, a deliberately sought after design feature to be more substitutionally inert. Possibly a larger lanthanide metal, able to accommodate L^1 and a monomer substrate, may represent an ideal ROP catalyst precursor.

Lanthanide(III) phenolate amide catalyst precursors, Ln = La (6) and Sm (7) containing the dianionic phenolate ligand, L^1. Indeed, attachment of the dianionic phenolate ligand, L^1 to larger lanthanide metals, such as samarium and lanthanum, drastically increased catalytic activity towards ROP of both L-lactide and ε-caprolactone compared with the less active ytterbium catalyst precursor (compound **8**). Quantitative polymer conversion was readily achieved with catalyst precursor **6** within 1 min at room temperature at a monomer–catalyst ratio of 100 : 1 (Table 2; entry 6 and Table 3; entry 7). Moreover, increasing L-lactide–catalyst **6** ratios from 100 : 1 up to 1000 : 1 readily afforded complete conversion to polylactide (the more challenging of the two cyclic monomers to polymerize) at room temperature within 10 min (Table 2, entries 7–10).

The samarium analogue, **7** displayed intermediate catalytic behaviour, between the larger, highly active lanthanum and the less active, smaller ytterbium compounds (Table 2; entry 11 and Table 3; entries 8–10). Finally, heating (80 °C) the L-lactide polymerization reaction with **7** (100 : 1) for 60 min only achieved moderate polymer conversion (35%), whilst significantly greater conversion to polycaprolactone (78%) was readily attained at room temperature under identical reaction conditions.

Polymer molecular weight distributions/compositions from catalyst precursors 6 and 7. Gel permeation chromatographic (GPC) analyses of the polylactide samples indicated formation of high molecular weight polymer. The polydispersities of all measured polymers are in the range 1.01–1.62; the upper ranges being indicative of transesterification[37] (Tables 2 and 3). Most notable is that longer polymerization reaction times produce broader molecular weight distributions (Table 2, entries 6 *vs.* 7) consistent with the notion that $k_{propagation} > k_{transesterification}$. This is a reasonable proposition (especially for intermolecular transesterification) since $k_{transesterification}$ requires collision of two large polyester oligomers whereas $k_{propagation}$ merely requires monomer and propagating chain collisions to occur. Extended polymerization reaction times, where quantitative polymer conversion has already ensued, allows the effect of slower transesterification reactions to become more significant, thereby affecting polymer polydispersity.

Obviously robust coordination of the multidentate, dianionic phenolate ligand $(L^1)^{2-}$ to lanthanide(III) metals provides a uniform, consistent catalytic pocket, or coordination environment, for monomer or polyester oligomers such that some of these subtle differences in polymer characteristics are detectable.

End-group analysis *via* ESI-MS of polylactide obtained from reaction of **6** with L-lactide (Table 2, entry 8) provides unequivocal evidence that the modified tridentate, dianionic phenolate ligand remains bound to the lanthanide metal center during polymerization reactions, and the labile monodentate nucleophilic amide group, $[N(SiMe_3)_2]$ is the preferred initiating group attached to the lanthanum metal (Fig. 4). However, polylactide cycles predominate (at least in low molecular weight fractions), which result from intra-moleuclar, intra-chain transesterification reactions. It is noteworthy that this mass spectrum is significantly different from that previously reported[37] for polylactide polymerized by the analogous $[La(L)_2(N(SiMe_3)_2)]$ where significant quantities of L was incorporated into the polymer.[37]

Finally, polymerization of *rac*-lactide (1 : 100 cat–monomer) in THF or toluene by catalyst precursor **6** was performed to assess the stereoselectivity. Unfortunately, this study indicated that there was no significant heterotactic bias in polymer formed using catalyst precursor **6** (Pr = 48.5% in toluene).

Kinetics analysis of ring-opening polymerization of L-lactide. Detailed studies of the kinetics of the L-lactide polymerization reaction with catalyst precursor **6** were conducted to establish reaction order in monomer and lanthanum catalyst precursor.

 This journal is © The Royal Society of Chemistry 2009

Published on 23 February 2009 on http://pubs.rsc.org | doi:10.1039/B821770J
Downloaded by UNIVERSITY OF BRIGHTON on 30/04/2013 12:15:14.

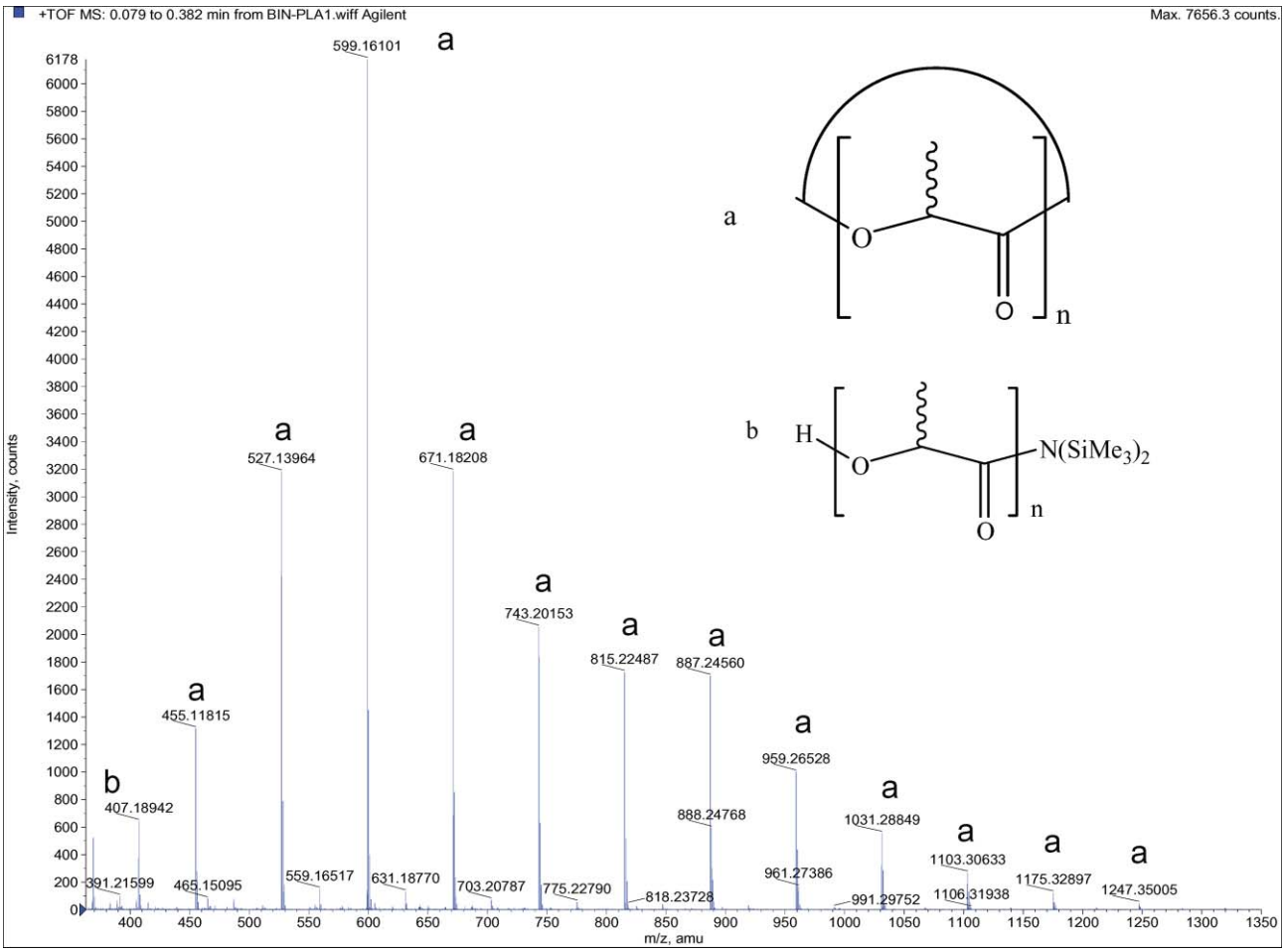

Fig. 4 ESI-MS of polymer produced from (Table 2, entry 8) indicating amide end-groups and polylactide cycles.

^{1}H NMR spectroscopy ($CDCl_3$) was used to determine polymer conversions (or monomer consumption). Several reactions were performed at room temperature where initial lactide concentration $[LA]_o$ (0.0694 M) was held constant and catalyst concentrations (1 : 300, 0.2313 mM; 1 : 400, 0.1735 mM; 1 : 500, 0.1388 mM; 1 : 600, 0.1156 mM; 1 : 750, 0.0925 mM) were varied until at least >85% conversion to polylactide was observed. First-order kinetics plots of $\ln([LA]_o/[LA]_t)$ *vs.* time were linear over all concentration ranges assessed, indicating that the polymerization proceeded with a first-order dependence on monomer concentration (Fig. 5). As a precautionary measure, second-order kinetic plots of $(1/[LA]_t - 1/[LA]_o)$ *vs.* time were plotted and, as anticipated, these were non-linear, supporting the first-order determination plotted above (ESI Fig. S7).†

From these data and a plot of k_{obs} *vs.* [**6**] (Fig. 6), the value of k was determined as 0.025 M^{-2} s^{-1} (note: $k_{obs} = k[\mathbf{6}]^x$, where k_{obs} is the *pseudo*-first-order rate constant and k is the overall propagation rate constant) such that the overall kinetic rate equation was determined: $-d[LA]/dt = k[LA]^1[\mathbf{6}]^1$.

GPC analyses of these polylactide samples obtained from kinetics analyses indicate good polymerization control as evidenced by a linear relationship between the number average molecular weight (M_n) and the initial lactide-to-initiator ratio ([M]/[I]) (Fig. 7).

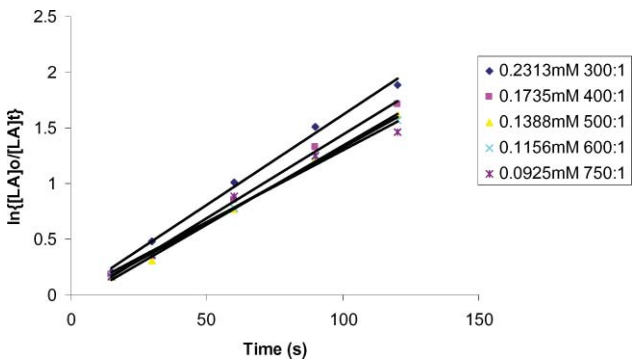

Fig. 5 First-order kinetic plots for L-lactide *vs.* time at various concentrations of **6**.

Furthermore, the PDIs are low, ranging from 1.19–1.63 compared to similar lanthanide complexes of monoanionic phenolate ligands reported previously.[37]

These kinetics findings are similar to those observed for the ring-opening polymerization of lactide by zinc alkoxide and yttrium silylamido complexes.[35,58] The first-order dependence on lactide is consistent with a mechanism which requires one molecule of lactide monomer per active site of the catalyst.

Downloaded by UNIVERSITY OF BRIGHTON on 30/04/2013 12:15:14.
Published on 23 February 2009 on http://pubs.rsc.org | doi:10.1039/B821770J

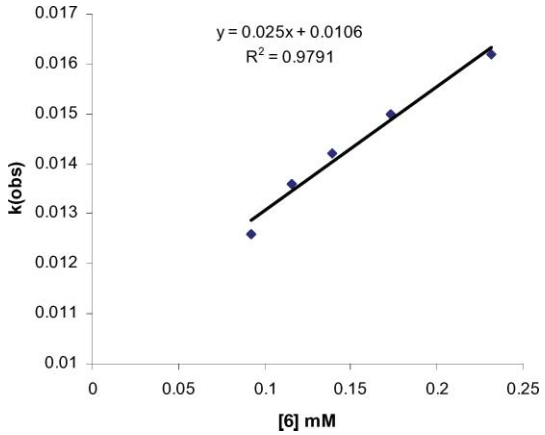

Fig. 6 Linear plot of k_{obs} *vs.* [**6**] for the polymerization of lactide.

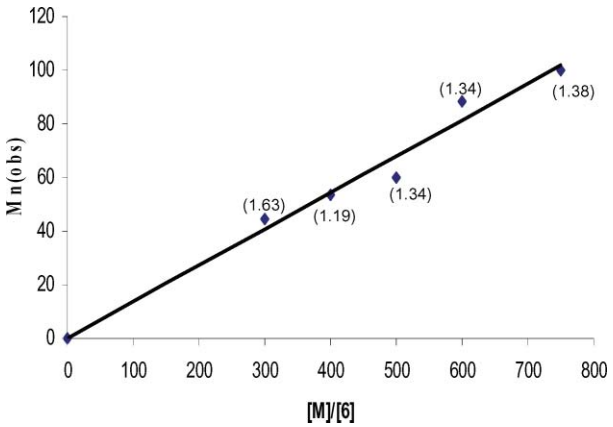

Fig. 7 Polymerization of L-lactide catalyzed by **6** in toluene at r.t. after 5 min displaying relationship between M_n(obs) of polymer and initial monomer to initiator ratio, [M]/[**6**] (NB: data obtained from kinetics studies, values in parenthesis are polydispersities).

Conclusions

A series of divalent and trivalent lanthanide complexes containing new tridentate [ONO] and tetradentate [ONNO] dianionic ligands has been synthesized and characterized. The trivalent compounds were synthesized by oxidation of the corresponding homoleptic divalent ytterbium compounds using mild oxidizing agents such as AgOTf and alcohols and by ligand exchange transamination reactions. The solid-state structure of **2** supports a dimeric divalent ytterbium complex containing five-coordinate centers; the fifth coordination is from a bridging phenoxide. Many of these compounds have moderate catalytic activity towards the ring-opening polymerization of L-lactide and ε-caprolactone, with **6** being an excellent initiator. Studies of the kinetics of L-LA polymerization by **6** revealed that the modified [ONO] tridentate, dianionic phenolate ligand $(L^1)^{2-}$ remains bound to the lanthanide metal center during polymerization reactions and accounted for the first-order consumption of L-lactide and good polymerization control.

Experimental

General

All air- or moisture-sensitive reactions were carried out under a dry nitrogen atmosphere, employing standard Schlenk line and drybox techniques. L-lactide and ε-caprolactone were purchased from Aldrich, purified by sublimation and distillation, respectively, and both were stored under an inert atmosphere. Solvents were dried over sodium/benzophenone and distilled under a nitrogen atmosphere. Deuterated solvents were purchased from Cambridge Isotope Laboratory, dried over sodium, deoxygenated and distilled by vacuum transfer. HL ligand,[38] H_2L^{II} ligand,[39] $[Ln(N(SiMe_3)_2)_3]$ (Ln = La, Sm, Yb)[59] and $[Yb(N(SiMe_3)_2)_2(THF)_2]$[60] were prepared and purified according to the indicated literature procedure. AgO_3SCF_3 and unsubstituted phenol were purchased from Acros, stored under an inert atmosphere, and were used as received. Melting points were obtained from sealed capillaries on a Mel-Temp apparatus and are uncorrected. IR spectra (4000–450 cm^{-1}) were recorded as KBr Nujol mulls on an ATI Mattson Genesis Series FTIR Spectrometer. All ^1H and ^{13}C NMR spectra were recorded on a Bruker AVANCE-500 NMR spectrometer and referenced to C_6D_5H, C_7D_7H or C_4D_7HO (^1H) and C_6D_6, C_7D_8 or C_4D_8O (^{13}C). Elemental analyses (sealed ampoules under inert atmosphere) were performed by Midwest Microlab, Indianapolis, IN. Single crystals, suitable for X-ray crystallography were sealed under an inert atmosphere in glass capillaries. Mass spectrometry was performed using high-resolution time of flight G1969A instrumentation (Agilent, Santa Clara, CA, USA). Samples (10 ppm) were dissolved in 10% THF and introduced to the MS using direct infusion at flow rate of 10 μL min^{-1} using acetic acid as an ionization agent. The positive ionization was performed at the voltage of 4000 V and with fragmentor set to 150 V. Nitrogen was used as the nebulizing (25 psi) and drying (7 L min^{-1}) gas at a temperature of 150 °C. The determinations were performed within the mass error of 10 ppm determined by the calibration prior to and after the measurement.

2,4-Di-*tert*-butyl-6-{[(2′-hydroxyethyl)methylamino]methyl}-phenol (H_2L^1) ligand

2,4-Di-*tert*-butylphenol (27.47 g, 133.1 mmol), 37 wt% formalin (4.0 g, 130 mmol), and 2-(methylamino)ethanol (10.00 g, 133.1 mmol) were dissolved in ethanol (100 mL). The resulting solution was heated at reflux for 16 h and then cooled to room temperature. Solvent was removed *via* rotary-evaporation to obtain pale yellow oil. Recrystallization from methanol at –20 °C yielded a white powder (21 g, 53%). Mp: 96–98 °C. (Found: C 73.6, H 10.55, N 4.8. $C_{18}H_{31}NO_2$ requires C 73.7, H 10.65, N 4.8%). $\tilde{\nu}_{max}/cm^{-1}$ 3201 s, 3105 s, 1759 w, 1604 m, 1315 m, 1242 vs, 1199 m, 1153 m, 1126 w, 1084 s, 1053 m, 1026 s, 929 m, 875 vs, 810 m, 760 w, 725 s, 667 w, 652 w, 578 w, 528 w, 509 w, 467 w, 416 w (Nujol). δ_H (500.1 MHz; C_6D_6; 298 K) 1.36 (9H, s, ^tBu), 1.70 (9H, s, ^tBu), 2.01 (3H, s, $ArCH_2NMe$), 2.31 (2H, t, *J* 5.6, NCH_2CH_2OH), 3.27 (2H, t, *J* 5.6, NCH_2CH_2OH), 3.35 (2H, s, $ArCH_2N$), 6.06 (1H, b, NCH_2CH_2OH), 7.07 (1H, s, Ar*H*), 7.50 (1H, s, Ar*H*), 10.76 (1H, b, ArO*H*). $\delta_{C\{H\}}$ (125.8 MHz; C_6D_6; 298 K) 30.4 (CMe_3), 32.3 (CMe_3), 34.7 (CMe_3), 35.7 (CMe_3), 41.8 ($ArCH_2NMe$), 51.9 ($NCH_2CH_2NMe_2$), 60.2 ($ArCH_2N$), 62.9 ($NCH_2CH_2NMe_2$), 122.3 (arom-CH), 123.5 (arom-CMe_3), 124.3

 This journal is © The Royal Society of Chemistry 2009

Downloaded by UNIVERSITY OF BRIGHTON on 30/04/2013 12:15:14.
Published on 23 February 2009 on http://pubs.rsc.org | doi:10.1039/B821770J

(arom-*C*H), 135.9 (arom-*C*Me$_3$), 141.2 (arom-*C*CH$_2$N), 155.4 (arom-*C*O).

[Yb(L^{I})]$_2$ (1). A deep orange hexanes solution (10 mL) of [Yb(N(SiMe$_3$)$_2$)$_2$(THF)$_2$] (0.32 g, 0.50 mmol) was treated with a colourless hexanes solution (10 mL) of H$_2$L^{I} ligand (0.15 g, 0.50 mmol) at room temperature and stirred overnight. Upon addition, the colour changed immediately to a deep red solution with deposition of **1** (0.21 g, 90%) as deep red crystals. Mp: 234–239 °C. (Found: C 46.3, H 6.4, N 3.25. $C_{36}H_{58}N_2O_4Yb_2$ requires C 46.55, H 6.3, N 3.0%); $\tilde{\nu}_{max}$/cm^{-1}: 1604 w, 1307 s, 1199 w, 1095 s, 972 w, 929 m, 887 m, 817 m, 771 w, 725 vs, 667 w (Nujol). δ_H (500.1 MHz; C_4D_8O; 298 K) –0.19 (3H, s, ArCH$_2$N*Me*), 0.90 (9H, s, ^{t}*Bu*), 1.14 (2H, b, NC*H*$_2$C*H*$_2$O), 1.29 (9H, s, ^{t}*Bu*), 1.55 (2H, b, NC*H*$_2$C*H*$_2$O), 2.31 (2H, s, ArC*H*$_2$NMe), 7.13 (1H, d, *J* 7.5 Ar*H*), 7.19 (1H, d, *J* 7.5 Ar*H*). δ_H (500.1 MHz; C_7D_8; 298 K) 0.76 (2H, s, ArC*H*$_2$NMe), 1.03 (2H, s, ArC*H*$_2$NMe), 1.13 (2H, b, NC*H*$_2$C*H*$_2$O), 1.61 (2H, b, NC*H*$_2$C*H*$_2$O), 1.21 (4H, b, NC*H*$_2$C*H*$_2$O), 1.29 (9H, b, ^{t}*Bu*), 1.35 (18H, s, ^{t}*Bu*), 1.41 (3H, s, ArCH$_2$N*Me*), 1.47 (3H, s, ArCH$_2$N*Me*), 1.79 (9H, s, ^{t}*Bu*), 6.72 (1H, s, Ar*H*), 7.45 (1H, s, Ar*H*), 8.88 (1H, s, Ar*H*), 9.15 (1H, s, Ar*H*); $\delta_{C\{H\}}$ (125.8 MHz; C_4D_8O; 298 K) 6.9 (*C*Me$_3$), 11.9(*C*Me$_3$), 14.6 (C*Me*$_3$), 23.7 (C*Me*$_3$), 30.1 (N*C*H$_2$*C*H$_2$NMe$_2$), 30.8 (N*C*H$_2$*C*H$_2$NMe$_2$), 32.7 (ArCH$_2$N*Me*), 33.8 (Ar*C*H$_2$N), 126.2 (arom-*C*CH$_2$N), 128.5 (arom-*C*Me$_3$), 128.9 (arom-*C*Me$_3$), 129.1 (arom-*C*H), 129.8(arom-*C*H), 155.1 (arom-*C*O).

[Yb(L^{II})]$_2$ (2). A deep orange hexanes solution (10 mL) of [Yb(N(SiMe$_3$)$_2$)$_2$(THF)$_2$] (0.32 g, 0.50 mmol) was treated with a colourless hexanes solution (10 mL) of H$_2$L^{II} ligand (0.26 g, 0.50 mmol) at room temperature and stirred overnight. Upon addition, the colour changed immediately to a deep red solution. Deep red crystals of **2** (0.32 g, 92%) were recrystallized from hexanes at –20 °C. Deep red single crystals of **2** suitable for X-ray crystallography were obtained from a toluene–hexanes solution at –20 °C. Mp: 200–204 °C. (Found: C 58.75, H 7.65, N 4.0. $C_{68}H_{108}N_4O_4Yb_2$ requires C 58.7, H 7.8, N 4.0%). $\tilde{\nu}_{max}$/cm^{-1}: 1604 s, 1304 vs, 1280 vs, 1261 vs, 1203 s, 1169 s, 1130 m, 1091 s, 1076 s, 1018 vs, 926 s, 875 s, 837 vs, 806 vs, 744 s, 671 m, 644 w, 609 m, 528 s, 430 m (Nujol). δ_H (500.1 MHz; C_4D_8O; 298 K) 0.99 (18H, s, ^{t}*Bu*), 1.22 (18H, s, ^{t}*Bu*), 1.81 (6H, s, ArCH$_2$N*Me*), 2.08 (4H, s, NC*H*$_2$C*H*$_2$N), 2.65 (4H, s, ArC*H*$_2$NMe), 6.45 (2H, s, Ar*H*), 6.93 (2H, s, Ar*H*). δ_H (500.1 MHz; C_7D_8; 298 K) 1.47 (9H, s, ^{t}*Bu*), 1.55 (9H, s, ^{t}*Bu*), 1.59 (9H, s, ^{t}*Bu*), 1.81 (3H, s, ArCH$_2$N*Me*), 1.99 (9H, s, ^{t}*Bu*), 2.28 (3H, s, ArCH$_2$N*Me*), 2.64 (1H, dd, *J* 11.0, NC*H*$_2$C*H*$_2$N), 2.67 (1H, dd, *J* 11.0, NC*H*$_2$C*H*$_2$N), 2.82 (1H, t, *J* 13.1, NC*H*$_2$C*H*$_2$N), 3.33 (1H, t, *J* 13.1, NC*H*$_2$C*H*$_2$N), 4.13 (2H, d, J 10.7, ArC*H*$_2$N), 4.17 (2H, d, J 10.7, ArC*H*$_2$N), 6.98 (1H, d, *J* 2.5, Ar*H*), 7.17 (1H, d, *J* 2.5, Ar*H*), 7.55 (1H, d, *J* 2.5, Ar*H*), 7.66 (1H, d, *J* 2.5, Ar*H*). $\delta_{C\{H\}}$ (125.8 MHz; C_4D_8O; 298 K) 29.9 (C*Me*$_3$), 30.6 (ArCH$_2$N*Me*), 32.2 (C*Me*$_3$), 34.0 (*C*Me$_3$), 35.6 (*C*Me$_3$), 42.8 (N*C*H$_2$*C*H$_2$N), 51.1 (Ar*C*H$_2$N), 123.3 (arom-*C*CH$_2$N), 125.7 (arom-*C*H), 131.2 (arom-*C*Me$_3$), 135.7 (arom-*C*Me$_3$), 138.1 (arom-*C*H), 165.8 (arom-*C*O). $\delta_{C\{H\}}$ (125.8 MHz; C_7D_8; 298 K) 30.0 (C*Me*$_3$), 31.9 (C*Me*$_3$), 32.2 (C*Me*$_3$), 32.4 (C*Me*$_3$), 34.0 (*C*Me$_3$), 34.1 (*C*Me$_3$), 35.3 (*C*Me$_3$), 35.7 (*C*Me$_3$), 37.7 (ArCH$_2$N*Me*), 43.7 (ArCH$_2$N*Me*), 50.1 (N*C*H$_2$*C*H$_2$N), 57.2 (N*C*H$_2$*C*H$_2$N), 62.9 (Ar*C*H$_2$N), 64.5 (Ar*C*H$_2$N), 121.9 (arom-*C*H), 124.9 (arom-*C*Me$_3$), 138.1 (arom-*C*H), 132.9 (arom-*C*Me$_3$), 158.6 (arom-*C*CH$_2$N), 168.8 (arom-*C*O).

[Yb(L$_2$)] (3). A deep orange hexanes solution (10 mL) of [Yb(N(SiMe$_3$)$_2$)$_2$(THF)$_2$] (0.32 g, 0.50 mmol) was treated with a colourless hexanes solution (10 mL) of HL ligand (0.32 g, 1.0 mmol) at room temperature and stirred overnight. Upon addition, the colour changed immediately to a dark green solution with deposition of **3** (0.38 g, 94%) as dark green crystals. Mp: 157–160 °C. (Found: C 58.9, H 8.6, N 6.8. $C_{40}H_{70}N_4O_2Yb$ requires C 59.2, H 8.7, N 6.9%). $\tilde{\nu}_{max}$/cm^{-1}: 1601 m, 1319 s, 1261 m, 1203 w, 1161 m, 1099 w, 1022 w, 968 w, 879 w, 802 w, 775 w, 725 vs (Nujol). δ_H (500.1 MHz; C_6D_6; 298 K) 1.38 (4H, b, NCH$_2$C*H*$_2$NMe$_2$), 1.55 (18H, s, ^{t}*Bu*), 1.69 (6H, s, ArCH$_2$N*Me*), 1.75 (18H, s, ^{t}*Bu*), 1.81 (6H, s, N*Me*$_2$), 1.98 (6H, s, N*Me*$_2$), 2.28 (2H, b, ArC*H*$_2$N), 2.86 (2H, b, NC*H*$_2$CH$_2$NMe$_2$), 2.94 (2H, b, NC*H*$_2$CH$_2$NMe$_2$), 4.10 (2H, b, ArC*H*$_2$N), 7.16 (2H, s, Ar*H*), 7.85 (2H, s, Ar*H*). $\delta_{C\{H\}}$ (125.8 MHz; C_6D_6; 298 K) 30.9 (C*Me*$_3$), 32.9 (C*Me*$_3$), 34.5 (N*Me*$_2$), 36.2 (N*Me*$_2$), 44.3 (*C*Me$_3$), 45.8 (*C*Me$_3$), 48.3 (N*C*H$_2$*C*H$_2$NMe$_2$), 50.6 (N*C*H$_2$*C*H$_2$NMe$_2$), 57.6 (ArCH$_2$N*Me*), 66.5 (Ar*C*H$_2$N), 123.3 (arom-*C*Me$_3$), 124.6 (arom-*C*H), 127.3 (arom-*C*H), 128.1 (arom-*C*Me$_3$), 132.4 (arom-*C*CH$_2$N), 166.0 (arom-*C*O).

[Yb(L^{I})(O$_3$SCF$_3$)(THF)] (4). A solution of THF (15 mL) was added at room temperature to a deep red powder of **1** (0.40 g, 0.43 mmol) and a white powder of AgO$_3$SCF$_3$ (0.22 g, 0.86 mmol) and stirred for 24 h. The resulting pale yellow solution was separated from the black silver metal and concentrated to yield a yellow solid, which was recrystallized from a mixture of THF–hexanes at 35 °C to afford **4** (0.33 g, 56%) as yellow powder. Mp: 216–219 °C. (Found: C 40.35, H 5.4, N 2.2. $C_{23}H_{37}F_3NO_6SYb$ requires C 40.3, H 5.4, N 2.0%). $\tilde{\nu}_{max}$/cm^{-1} 1612 m, 1593 m, 1462 vs, 1373 s, 1311 vs, 1257 vs, 1196 vs, 1080 s, 1030 vs, 972 w, 895 w, 876 m, 841 m, 802 s, 748 w, 725 w, 679 w, 644 s, 609 w, 517 w, 494 w, 463 w (Nujol).

[Yb(L^{I})(OPh)] (5). Phenol (0.15 g, 1.6 mmol) was added to a deep red THF (15 mL) solution of **1** (0.46 g, 0.50 mmol) at room temperature and stirred overnight. The solution gradually turned into a pale yellow solution, after which time all volatiles were removed *in vacuo*, to yield a yellow powder of **5** (0.38 g, 68%). Mp: 210–213 °C. (Found: C 52.0, H 6.5, N 2.4. $C_{24}H_{34}NO_3Yb$ requires (for no THF) C 51.7, H 6.15, N 2.5%; $C_{28}H_{42}NO_4Yb$ requires (for 1 THF) C 53.4, H 6.7, N 2.2%). $\tilde{\nu}_{max}$/cm^{-1} 1589 s, 1461 vs, 1377 s, 1311 s, 1288 m, 1246 s, 1203 w, 1165 m, 1134 w, 1084 s, 1022 m, 926 w, 895 w, 875 w, 841 m, 810 m, 764 m, 725 w, 694 m, 656 w, 613 w, 571 w, 536 w, 490 w, 459 w (Nujol).

[La(L^{I})(N(SiMe$_3$)$_2$)(THF)$_2$] (6). H$_2$L^{I} ligand (0.59 g, 2.0 mmol) in THF (20 mL) was added to a THF (20 mL) solution of [La(N(SiMe$_3$)$_2$)$_3$] (1.24 g, 2.00 mmol) at –40 °C *via* a cannula. The resulting colourless reaction mixture was stirred gently and warmed to room temperature (18 h) to afford a pale yellow solution of **6**. Volatiles were removed *in vacuo*, and the compound was recrystallized from hexanes at 25 °C and dried to give **6** as a pale yellow powder (0.75 g, 51%). Mp: 218–222 °C. (Found: C 52.5, H 8.8, N 3.7. $C_{32}H_{63}LaN_2O_4Si_2$ requires C 52.3, H 8.6, N 3.8%). $\tilde{\nu}_{max}$/cm^{-1} 1604 w, 1307 m, 1261 s, 1199 w, 1153 m, 1088 vs, 1026 vs, 972 w, 933 w, 883 w, 802 s, 725 s (Nujol). δ_H (500.1 MHz; C_4D_8O; 348 K) –0.08 (18H, s, SiMe$_3$), 1.30 (9H, s, ^{t}*Bu*), 1.45 (9H, s, ^{t}*Bu*), 2.02 (3H, s, ArCH$_2$N*Me*), 2.44 (4H, b, NC*H*$_2$C*H*$_2$O), 4.07 (2H, b, ArC*H*$_2$N), 6.66 (1H, s, ArH), 6.98 (2H, s, ArH). δ_H (500.1 MHz; C_6D_6; 323 K) 0.18 (18H, s, Si*Me*$_3$), 0.87 (2H, s,

Downloaded by UNIVERSITY OF BRIGHTON on 30/04/2013 12:15:14.
Published on 23 February 2009 on http://pubs.rsc.org | doi:10.1039/B821770J

ArCH_2NMe), 0.88 (3H, s, ArCH$_2$NMe), 1.25 (9H, s, ^{t}*Bu*), 1.41 (9H, b, ^{t}*Bu*), 1.45 (8H, b, THF), 1.67 (1H, b, NCH_2CH_2O), 1.92 (1H, b, NCH_2CH_2O), 2.19 (1H, b, NCH_2CH_2O), 2.50 (1H, b, NCH_2CH_2O), 3.60 (8H, b, THF), 7.00 (1H, s, ArH), 7.45 (1H, s, ArH). $\delta_{C\{H\}}$ (125.8 MHz; C_4D_8O; 298 K) 6.9 ($SiMe_3$), 26.5 (CMe_3), 30.8 (ArCH$_2$NMe), 38.8 (CMe_3),34.3 (NCH_2CH_2NMe$_2$), 36.0 (NCH_2CH_2NMe$_2$), 43.9 (CMe_3), 52.4 (CMe_3), 64.4 (ArCH_2N), 122.7 (arom-CH), 126.5 (arom CMe_3), 129.2 (arom-CH), 129.7 (arom-CMe_3), 136.3 (arom-CCH$_2$N), 167.9 (arom-CO). $\delta_{C\{H\}}$ (125.8 MHz; C_6D_6; 298 K) 3.0 (SiMe_3), 7.2 (ArCH$_2$NMe), 12.0 (CMe_3), 14.7 (CMe_3), 21.2 (CMe_3), 23.4 (CMe_3), 26.0 (THF), 32.3 (ArCH_2N), 32.7 (NCH_2CH_2NMe$_2$), 35.3 (NCH_2CH_2NMe$_2$), 68.3 (THF), 127.9 (arom-CH), 128.1 (arom-CMe_3), 128.2 (arom-CH), 128.7 (arom-CMe_3), 129.0 (arom-CCH$_2$N), 162.4 (arom-CO).

[Sm(L^I)(N(SiMe$_3$)$_2$)(THF)] (7). H_2L^I ligand (0.59 g, 2.0 mmol) in THF (20 mL) was added to a THF (20 mL) solution of [Sm(N(SiMe$_3$)$_2$)$_3$] (1.26 g, 2.00 mmol) at –40 °C *via* a cannula. The resulting reaction mixture was stirred gently and warmed to room temperature (18 h) to afford a pale yellow cloudy solution of **7**. Volatiles were removed *in vacuo* with the resulting pale yellow solid being washed twice with hexanes and dried to afford **7** as a pale yellow powder (0.73 g, 54%). Mp: 217–220 °C. (Found: C 50.25, H 8.0, N 4.1. $C_{28}H_{55}N_2O_3Si_2Sm$ requires C 49.9, H 8.2, N 4.15%). $\tilde{\nu}_{max}$/cm^{-1} 1743 w, 1597 m, 1307 s, 1261 s, 1199 w, 1157 m, 1076 s, 1022 s, 972 w, 933 w, 887 w, 837 m, 806 m, 771 w, 725 vs, 601 w, 524 w (Nujol). δ_H (500.1 MHz; C_6D_6; 298 K) –1.67 (18H, s, SiMe_3), 0.21 (9H, s, ^{t}*Bu*), 0.30 (2H, s, ArCH_2N), 0.97 (4H, b, NCH_2CH_2O), 1.49 (4H, b, THF), 2.00 (9H, b, ^{t}*Bu*), 2.32 (3H, b, ArCH$_2$NMe), 3.56 (4H, b, THF), 7.65 (1H, s, ArH), 8.12 (1H, s, ArH).

[Yb(L^I)(N(SiMe$_3$)$_2$(THF)] (8). H_2L^I ligand (0.59 g, 2.0 mmol) in THF (20 mL) was added to a THF (20 mL) solution of [Yb(N(SiMe$_3$)$_2$)$_3$] (1.31 g, 2.00 mmol) at –40 °C *via* a cannula. The reaction mixture was stirred and warmed to room temperature (18 h) to afford a pale yellow cloudy solution of **8**. Volatiles were removed *in vacuo* with the resulting pale yellow solid being washed with hexanes and dried to afford **8** as a pale yellow powder, which was later recrystallized from toluene at 35 °C (0.72 g, 52%). Mp: 220–224 °C. (Found: C 49.0, H 7.8, N 3.4. $C_{28}H_{55}N_2O_3Si_2Yb$ requires (for 1 THF) C 48.25, H 7.95, N 4.0%); (Found: C 51.65, H 7.3, N 3.6. $C_{31}H_{55}N_2O_2Si_2Yb$ requires (for 1 molecule of toluene) C 51.9, H 7.7, N 3.9%). $\tilde{\nu}_{max}$/cm^{-1}: 1604 w, 1458 vs, 1377 s, 1307 s, 1273 s, 1242 m, 1203 w, 1165 m, 1126 w, 1080 s, 1045 m, 976 m, 914 w, 891 m, 833 m, 910 m, 771 w, 740 m, 725 m, 644 w, 605 m, 567 w, 605 w, 567 w, 528 w, 440 w (Nujol).

Typical polymerization reactions of L-LA or ε-CL

The appropriate quantity of catalyst precursor (*e.g.* 0.00347 mmol for L-LA 1 : 100; 0.0044 mmol for ε-CL 1 : 100) in toluene (0.5 mL) was added to a toluene (4.5 mL) solution of L-LA (50 mg, 0.347 mmol) or ε-CL (50 mg, 0.44 mmol) at the requisite temperature in a Schlenk flask *via* syringe. After an appropriate time (see Tables 2 and 3), an aliquot (*ca.* 0.5 mL) was taken from the reaction mixture and evaporated to dryness. ^{1}H NMR spectroscopy ($CDCl_3$) was used to determine the percentage of polymer conversion.

Kinetics analyses (from ROP of L-lactide using **6**) were obtained from room temperature toluene (4.5 mL) solutions of L-LA (50 mg, 0.347 mmol) to which the appropriate amount of catalyst (1 : 300, 0.2313 mM; 1 : 400, 0.1735 mM; 1 : 500, 0.1388 mM; 1 : 600, 0.1156 mM; 1 : 750, 0.0925 mM) in toluene (0.5 mL) was added *via* syringe. Aliquots (*ca.* 0.3 mL) (see Fig. 5–7) were taken from the reaction mixture and evaporated to dryness until >85% polymer conversion was attained. ^{1}H NMR spectroscopy ($CDCl_3$) was used to determine % polymer conversion. GPC analyses were measured using a Waters 1525 Binary HPLC pump coupled to two 7/8 × 300 mm Styragel® HR4 columns and a Waters 40 Differential Refractometer. The eluent was HPLC grade THF running at 1 mL min^{-1} (sample concentration 0.1% w/v THF). Polystyrene standards were used for calibration of the instrument. Breeze® software was used for peak analyses and calibration procedures. GPC was performed on polylactide samples from kinetics studies and 1 : 100 catalyst–monomer polymerization reactions.

X-Ray crystallography-structure determination

Data were collected using an Oxford Diffraction Gemini diffractometer (ω-scans) with Mo Kα radiation. The structure was solved by direct methods using Sir-92[61] and, following empirical absorption corrections, was refined with full-matrix least squares based on F^2 using SHELX-97.[62] All hydrogen atoms were added at calculated positions and refined by use of a riding model with isotropic displacement parameters based on the displacement parameter of the parent atom. Anisotropic displacement parameters were employed throughout for the non-hydrogen atoms.

Crystal refinement data

[YbL^{II}]$_2$ (2). $C_{68}H_{108}N_4O_4Yb_2.2(C_7H_8)$, M = 1575.94, red plates, monoclinic, space group $C2/c$, a = 28.8197(4), b = 9.0269(1), c = 30.2320(5) Å, β = 91.433(1)°, V = 7862.47(19) Å^3; D_c (Z = 4) = 1.331 Mg m^{-3}; μ(Mo Kα) = 2.413 mm^{-1}; specimen: 0.48 × 0.28 × 0.15 mm; $T_{min/max}$ = 0.786/1; T 100(2) K, $2\theta_{max}$ = 63.4°, 49 880 reflections collected of which 12 724 were unique (R_{int} = 0.050); R_1 = 0.054, wR_2 = 0.067 (all data); R_1 = 0.032, wR_2 = 0.064 ($I > 2\sigma(I)$), GOF = 0.91; $|\rho_{max}|$ = 2.1 e Å^{-3}.

Acknowledgements

We are very grateful to Kirtipal Barse and Dr Edward Kolodka, Josef Beranek and Dr Alena Kubatova at the University of North Dakota, for assistance with GPC data and TOF MS, respectively. Financial support from ND EPSCoR program and UND's chemistry department is gratefully acknowledged. The work on TOF MS was supported by the National Science Foundation under grant no. CHE-0216038.

Notes and references

1 G. G. Skvortsov, M. V. Yakovenko, P. M. Castro, G. K. Fukin, A. V. Cherkasov, J. F. Carpentier and A. A. Trifonov, *Eur. J. Inorg. Chem.*, 2007, 3260.
2 A. A. Trifonov, G. G. Skvortsov, D. M. Lyubov, N. A. Skorodumova, G. K. Fukin, E. V. Baranov and V. N. Glushakova, *Chem.–Eur. J.*, 2006, **12**, 5320.
3 D. Heitmann, C. Jones, P. C. Junk, K. A. Lippert and A. Stasch, *Dalton Trans.*, 2007, 187.
4 F. Yuan, Y. Zhu and L. Xiong, *J. Organomet. Chem.*, 2006, **691**, 3377.

 This journal is © The Royal Society of Chemistry 2009

View Article Online

5 Y. Yao, Z. Zhang, H. Peng, Y. Zhang, Q. Shen and J. Lin, *Inorg. Chem.*, 2006, **45**, 2175.
6 L. F. Sanchez-Barba, D. L. Hughes, S. M. Humphrey and M. Bochmann, *Organometallics*, 2006, **25**, 1012.
7 P. B. Hitchcock, M. F. Lappert and S. Tian, *J. Chem. Soc., Dalton Trans.*, 1997, 1945.
8 L. F. Sanchez-Barba, D. L. Hughes, S. M. Humphrey and M. Bochmann, *Organometallics*, 2005, **24**, 3792.
9 F. M. Kerton, A. C. Whitwood and C. E. Willans, *Dalton Trans.*, 2004, 2237.
10 N. K. Dutt and K. Nag, *J. Inorg. Nucl. Chem.*, 1968, **30**, 2779.
11 H. X. Li, Y. J. Zhu, M. L. Cheng, Z. G. Ren, J. P. Lang and Q. Shen, *Coord. Chem. Rev.*, 2006, **250**, 2059.
12 J. P. Collin, V. Heitz, S. Bonnet and J. P. Sauvage, *Inorg. Chem. Commun.*, 2005, **8**, 1063.
13 E. E. Delbridge, D. T. Dugah, C. R. Nelson, B. W. Skelton and A. H. White, *Dalton Trans.*, 2007, 143–153; D. T. Dugah, B. W. Skelton and E. E. Delbridge, *Dalton Trans.*, 2009, 1436–1443.
14 X. Xu, M. Ma, Y. Yao, Y. Zhang and Q. Shen, *Eur. J. Inorg. Chem.*, 2005, 676–684.
15 A. Lendlein, A. M. Schmidt, M. Schroeter and R. Langer, *J. Polym. Sci. Pol. Chem.*, 2005, **43**, 1369.
16 A. Amgoune, C. M. Thomas, T. Roisnel and J. F. Carpentier, *Chem.–Eur. J.*, 2005, **12**, 169.
17 H. Guo, H. Zhou, Y. Yao, Y. Zhang and Q. Shen, *Dalton Trans.*, 2007, 3555.
18 P. I. Binda, E. E. Delbridge, D. T. Dugah, B. W. Skelton and A. H. White, *Z. Anorg. Allg. Chem.*, 2008, **634**, 325–334.
19 S. Cotton, *Lanthanide and Actinide Chemistry*, John Wiley and Sons Ltd., 2006, pp. 1–143.
20 G. A. Molander and E. D. Dowdy, *J. Org. Chem.*, 1999, **64**, 6515–6517.
21 H. C. Aspinall, *Chem. Rev.*, 2002, **102**, 1807–1850.
22 K. C. Hultzsch, P. Voth, K. Beckerle, T. P. Spaniol and J. Okuda, *Organometallics*, 2000, **19**, 228–243.
23 J. Kido and Y. Okamoto, *Chem. Rev.*, 2002, **102**, 2357–2368.
24 P. Coppo, M. Duati, V. N. Kozhevnikov, J. W. Hofstraat and L. De Cola, *Angew. Chem., Int. Ed.*, 2005, **44**, 1806–1810.
25 L. Benisvy, P. Gamez, W. T. Fu, H. Kooijman, A. L. Spek, A. Meijerink and J. Reedijk, *Dalton Trans.*, 2008, 3147–3149.
26 J. Massue, S. J. Quinn and T. Gunnlaugsson, *J. Am. Chem. Soc.*, 2008, **130**, 6900–6901.
27 X. Yang, R. A. Jones and W.–K. Wong, *Dalton Trans.*, 2008, 1676–1678.
28 S. Claudel-Gillet, J. Steibel, N. Weibel, T. Chauvin, M. Port, I. Raynal, E. Toth, R. F. Ziessel and L. J. Charbonniere, *Eur. J. Inorg. Chem.*, 2008, 2856–2862.
29 Y.–W. He and C.–S. Loh, *Plant Sci.*, 2000, **159**, 117–124.
30 W. J. Evans, *Coord. Chem. Rev.*, 2000, **206–207**, 263–283.
31 Y. Yao, M. Ma, X. Xu, Y. Zhang, Q. Shen and W. T. Wong, *Organometallics*, 2005, **24**, 4014–4020.
32 C. X. Cai, A. Amgoune, C. W. Lehmann and J. F. Carpentier, *Chem. Commun.*, 2004, 330–331.
33 M. Deng, Y. Yao, Q. Shen, Y. Zhang and J. Sun, *Dalton Trans.*, 2004, 944.
34 J. Ling, W. Zhu and Z. Shen, *Macromolecules*, 2004, **37**, 758.
35 H. Ma and J. Okuda, *Macromolecules*, 2005, **38**, 2665–2673.
36 H. Ma, T. P. Spaniol and J. Okuda, *Dalton Trans.*, 2003, 4770.
37 P. I. Binda and E. E. Delbridge, *Dalton Trans.*, 2007, 4685–4692.
38 C. K. Williams, L. E. Breyfogle, S. K. Choi, W. Nam, V. G. Young, Jr., M. A. Hillmyer and W. B. Tolman, *J. Am. Chem. Soc.*, 2003, **125**, 11350–11359.
39 J. Balsells, P. J. Carroll and P. J. Walsh, *Inorg. Chem.*, 2001, **40**, 5568.
40 S. Bambirra, A. Meetsma and B. Hessen, *Organometallics*, 2006, **25**, 3454–3462.
41 H. Ma, T. P. Spaniol and J. Okuda, *Inorg. Chem.*, 2008, **47**, 3328–3339.
42 P. Voth, S. Arndt, T. P. Spaniol, J. Okuda, L. J. Ackerman and M. L. H. Green, *Organometallics*, 2003, **22**, 65–76; X. Chen, S. Lim, C. E. Plečnik, S. Liu, B. Du, E. A. Meyers and S. G. Shore, *Inorg. Chem.*, 2004, **43**, 692–698.
43 O. Dechy-Cabaret, B. Martin-Vaca and D. Bourissou, *Chem. Rev.*, 2004, **104**, 6147–6176.
44 S. Jacobsen, H. G. Fritz, P. Degrée, P. Dubois and R. Jérôme, *Ind. Crops Prod.*, 2000, **11**, 265–275.
45 Y. Ikada and H. Tsuji, *Macromol. Commun.*, 2000, **21**, 117.
46 N. Isogai, S. Asamura, T. Hagishi, Y. Ikada, S. Morita, J. Hillyer and W. J. Landis, *Tissue Eng.*, 2004, **10**, 673–687.
47 B. C. Benicewicz and P. K. Hopper, *J. Bioactive Comput. Polym.*, 1991, **6**, 64.
48 A. U. Daniels, M. K. O. Chang and K. P. Adriano, *J. Appl. Biomater.*, 1990, **1**, 57.
49 K. A. Athanasiou, G. G. Niederauer and C. M. Agrawal, *Biomaterials*, 1996, **17**, 93.
50 R. Langer, *Nature*, 1998, **392**, 5.
51 K. E. Uhrich, S. M. Cannizzaro, R. S. Langer and K. M. Shakesheff, *Chem. Rev.*, 1999, **99**, 3181.
52 M. Jacoby, *Chem. Eng. News*, 2001, **79**, 30.
53 J. Panyam and V. Labhasetwar, *Adv. Drug Delivery Rev.*, 2003, **55**, 329.
54 L. Mu and S. S. Feng, *J. Controlled Release*, 2003, **86**, 33.
55 R. Langer, *Science*, 2001, **293**, 58–59.
56 R. Langer and N. A. Peppas, *AIChE J.*, 2003, **49**, 2990–3006.
57 R. Langer and D. A. Tirrell, *Nature*, 2004, **428**, 487–492.
58 J. C. Wu, B. H. Huang, M. L. Hsueh, S. L. Lai and C. C. Lin, *Polymer*, 2005, **46**, 9784–9792.
59 W. A. Herrmann, *Synthetic Methods of Organometallic and Inorganic Chemistry: Lanthanides and Actinides*, ed. F. T. Edelmann, Thieme Verlag Stuttgart, New York, 1997, vol. 6, pp. 37–40.
60 W. J. Evans, D. K. Drummond, H. Zhang and J. L. Atwood, *Inorg. Chem.*, 1998, **27**, 575.
61 A. Altomare, G. Cascarano, G. Giacovazzo, A. Guagliardi, M. C. Burla, G. Polidori and M. Camalli, *J. Appl. Crystallogr.*, 1994, **27**, 435.
62 G. M. Sheldrick, *Acta Crystallogr., Sect. A: Found. Crystallogr.*, 2008, **64**, 112–122.

Published on 23 February 2009 on http://pubs.rsc.org | doi:10.1039/B821770J
Downloaded by UNIVERSITY OF BRIGHTON on 30/04/2013 12:15:14.